7744 *Macromolecules* **2010**, *43*, 7744–7751
DOI: 10.1021/ma1009484

Macromolecules
ARTICLE

Bidimensional Response Maps of Adaptive Thermo- and pH-Responsive Polymer Brushes

Xavier Laloyaux,* Bertrand Mathy, Bernard Nysten, and Alain M. Jonas*

Bio and Soft Matter, Institute of Condensed Matter and Nanosciences, Université catholique de Louvain, Croix du Sud 1 box 4, 1348 Louvain-la-Neuve, Belgium

Received April 29, 2010; Revised Manuscript Received June 18, 2010

ABSTRACT: We depict the collapse transition of adaptive thermo- and pH-responsive copolymer brushes based on poly(di(ethylene glycol) methyl ether methacrylate-*co*-methacrylic acid) random copolymer chains (P(MEO_2MA-*co*-MAA)) by drawing bidimensional (2D) maps of the swelling ratio versus temperature and pH for different brush compositions. The collapse transition is probed by quartz crystal microbalance measurements with dissipation monitoring (QCM-D). While P(MEO_2MA) brushes exhibit a thermo-collapse transition around 22 °C and P(MAA) brushes display a pH-induced collapse transition at pH = 5.5, P(MEO_2MA-*co*-MAA) brushes undergo a collapse transition modulated by either temperature or pH from a swollen state at low temperature and high pH to a collapsed state at high temperature and low pH. By varying the composition of the copolymer in MAA units from 4 to 14 mol %, the brushes switch from a pH-modulated thermo-responsive behavior to a temperature-modulated pH-responsive behavior in water. The 2D maps of swelling ratio also illustrate the complex interplay between pH and temperature, and provide a unique view of the response of adaptive brushes.

Introduction

Stimuli-responsive polymers are materials able to respond in a controlled and predictable manner to external triggers such as temperature, pH, or ionic strength. When grafted on a substrate in a dense brush, responsive polymers can be used to tune on demand surface adhesion, wetting behavior, or interfacial viscoelastic properties.[1−3] This variable tuning most often results from a sudden modification of the degree of swelling of the brush when the external trigger is varied over a limited range. The rapid variations of properties which result from the rapidly changing swelling ratio make responsive polymer brushes ideally suited for applications such as sensors,[4] microfluidic devices,[5−7] drug delivery systems,[8,9] actuation devices,[10] or tunable adhesive surfaces.[11,12]

Multiresponsive polymer brushes are coatings for which two or more triggers can be simultaneously applied in order to induce a tunable response. These systems, which are also called adaptive polymer brushes,[13,14] exhibit a response to a first stimulus which can be finely tuned by the use of a second trigger. For instance, a thermo- and pH-adaptive polymer brush can be obtained by the copolymerization of monomers whose homopolymers in solution demonstrate pH- or temperature-responsive phase behavior in the temperature range of interest.[15] Thermo-responsive homopolymers display a lower critical solution temperature (LCST) in water. At low temperatures, grafted thermo-responsive polymer chains swell and stretch away from the surface. When temperature increases above the collapse transition temperature, such brushes expel water and collapse on the substrate. pH-responsive polymer brushes are made of weak polyelectrolytes of charge varying with pH. Electrostatic repulsion can thus be modified by pH, resulting in differential swelling. The combination of both monomers in a single copolymer brush offers opportunities to promote or inhibit the thermal response depending on pH, provided the proper balance between the two effects is achieved by adjusting the copolymer composition or structure. This type of adaptive polymer brush could for instance be used in smart biological devices releasing a drug depending on the local temperature and/or pH of the human body.

Some adaptive polymers are homopolymers, among which the well-known poly((2-dimethylamino)ethyl methacrylate), PDMAEMA. PDMAEMA brushes are weak polybase brushes exhibiting a thermal collapse transition temperature which can be set from 40 to 80 °C depending on pH and salt concentration.[16−18] Such homopolymer brushes are thus adaptive; however, their collapse occurs only over a restricted temperature range. In order to extend the range of tunability, block copolymer brushes have been reported, such as poly(*N*-isopropylacrylamide-*block*-methacrylic acid), P(NIPAM-*b*-MAA).[15,19] This copolymer exhibits a wide range of collapse transition temperatures depending on its content in MAA and on the pH of the solution.[20] However, experimental[21] and theoretical[22] results show that such block copolymers brushes are composed of microdomains, which make their collapse transition complex.

Recently, we have reported on the synthesis of thermoresponsive *random* copolymer brushes based on di(ethylene glycol) methyl ether methacrylate (MEO_2MA) and (ethylene glycol) methyl ether methacrylate (OEGMA) and shown how the collapse transition of these brushes could be finely tuned in the physiological range by adjusting the copolymer composition.[23] These brushes exhibit properties similar to PNIPAM brushes but are much easier to grow in a controlled way by atom transfer radical polymerization (ATRP) and should not suffer from the slight cytotoxicity reported for PNIPAM.[24] Application of such brushes to control cell attachment[12] and bactericidal properties[25,26] has been demonstrated. Here, we report on the tuning of the thermal collapse of P(MEO_2MA)-based brushes by copolymerization in the presence of methacrylic acid (MAA), which provides pH sensitivity (Scheme 1). We follow in detail the collapse transition of such adaptive brushes over a large temperature and

*To whom correspondence should be addressed. E-mail: xavier.laloyaux@uclouvain.be (X.L.); alain.jonas@uclouvain.be (A.M.J.).

 Published on Web 08/30/2010

Scheme 1. General Chemical Formula of P((MEO$_2$MA)$_x$-*co*-(MAA)$_y$) Copolymer Brushes Containing *x* mol % of MEO$_2$MA and *y* mol % of MAA Content, Grown by ATRP from Si Surfaces

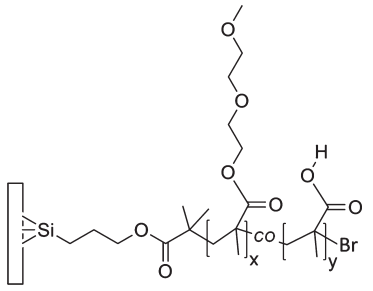

pH range by quartz crystal microbalance with dissipation monitoring measurements (QCM-D). QCM-D has been used before to monitor the thermal collapse transition of polymer brushes.[27] The acoustic thickness of polymer brushes can be obtained from the QCM-D data,[28] which provides access to the global conformation of the copolymer chains, swollen or collapsed depending on temperature. The method is extended here to follow the pH-response of polyacid brushes and the temperature- and pH-dependent collapse of P(MEO$_2$MA-*co*-MAA) adaptive brushes. The paper is structured in the following way: after the Experimental Section, we first characterize the composition of the copolymer brushes and estimate reactivity ratios. Then, the thermo- and pH-collapse transitions are investigated depending on the composition of the copolymer brushes, and a bidimensional diagram of acoustic thickness is presented, providing a unique view of the complex swelling of the brushes.

Experimental Section

Materials. 2-(2-Methoxyethoxy)ethyl methacrylate (MEO$_2$MA) and methacrylic acid (MAA) were purchased from Aldrich and used as received. Absolute ethanol was from Fluka. Milli-Q water (resistivity: 18.2 MΩ cm) was obtained from a Millipore system. Copper(I) chloride (99.995+%) (Cu^ICl), copper(II) chloride (99.999+%) ($Cu^{II}Cl_2$), and 2,2′-bipyridyl (99+%) (bipy) were provided by Aldrich. Benzyldimethylmonochlorosilane was from ABCR. Single-side polished silicon wafers (⟨100⟩ orientation) were from ACM (France). Quartz crystal sensors covered by a layer of SiO_2 (QSX 303) were purchased from Q-Sense (Sweden) and rinsed by ethanol before use. The different steps of the surface preparation are described below and are identical for silicon wafers and the QCM-D sensors, unless stated otherwise.

Brush Growth. Brushes were grown according to a protocol published before.[23] Briefly, the substrates were cleaned in a piranha solution (Si wafers) or by UV/ozone cleaning for 30 min (quartz sensors) (*caution: piranha solution is extremely corrosive*). The substrates were then silanized with an ATRP silane initiator (2-bromo-2-methylpropionic acid 3-trichlorosilanylpropyl ester) as described previously;[23] the thickness of the initiator monolayer was determined by X-ray reflectometry to be 1.1 ± 0.2 nm. For some experiments, a dilution of the initiator monolayer was achieved by mixing the silane initiator with known amounts of an inert silane, benzyldimethylchlorosilane. Different series of polymer brushes were synthesized by controlled radical polymerization. Controlled living polymerization conditions were attained for concentrations of monomers/bipy/CuCl/$CuCl_2$ = 190/5/1.6/0.08 mmol in a solution of ethanol (10 mL) and Milli-Q water (15 mL). For each series of brushes, a set of initiator-covered silicon substrates were immersed in the feed solution in an oxygen-free atmosphere (Schlenk tubes) and removed at increasing times to check the polymerization kinetics. When the ellipsometry-determined thickness reached about 100 nm, the polymerization was stopped and the resulting ∼100 nm thick brush was used for further experiments. The brush growth rates on silicon substrates and QCM-D sensors were similar. The grafting density of P(MEO$_2$MA) brushes was evaluated previously to be ∼0.33 nm^{-2} [29] and should be similar for the brushes grown from the undiluted silane layer.

Ellipsometry. The dry film thickness was measured with a spectroscopic ellipsometer (Uvisel from Horiba-Jobin-Yvon, France) at an incidence angle of 70° and in a wavelength range from 400 to 850 nm. The ellipsometric data were fitted by the DeltaPsi 2 software of the apparatus. The ellipsometric model consists of three layers: silicon (bulk), native silicon oxide (1.5 nm thickness), and polymer brush. The complex index of refraction of Si and native SiO_2 were taken from tabulated data provided by the manufacturer. The complex index of refraction of the brushes, $n - jk$, was modeled by a transparent Cauchy layer with $n(\lambda) = A + B\lambda^{-2} + C\lambda^{-4}$ and $k(\lambda) = 0$, with A, B, and C three fitted parameters. The measurement was carried out three times at different spots on the substrate. For a few samples, the evaluated ellipsometric thickness of the polymer brushes was compared to the thickness measured by X-ray reflectometry (experimental conditions are described in ref 28): both measurements generally agreed within better than 10%. The brush thickness on the QCM-D sensor was likewise evaluated by a model using four layers: gold, titanium, silicon oxide, and polymer layer (Cauchy layer). The values of index of refraction for Ti, Au, and SiO_2 were again tabulated values.

Quartz Crystal Microbalance with Dissipation Monitoring (QCM-D). QCM-D measurements were performed in water with a Q-Sense E4 microbalance. The AT-cut quartz crystal sensor of 14 mm diameter was oscillating at its fundamental frequency (5 MHz). All overtones were acquired, although the third overtone was generally selected for analysis unless mentioned otherwise. The thickness of the silicon oxide layer covering the sensor was evaluated by ellipsometry on five different sensors to be 23 ± 2.5 nm. The quartz sensor was mounted in a flow module with one side exposed to the solution. The module temperature was maintained with a precision of 0.02 °C. Data collection was realized in two ways: static (pH response) and dynamic (temperature response). For static measurements, three phosphate and three acetate buffer solutions (concentration = 0.05 M) added with NaCl to reach an ionic strength of 0.2 M were prepared at room temperature and were injected in the module for at least 45 min before performing the acquisition at a given temperature. For dynamic measurements, the temperature was ramped at 0.2 °C/min while continuously acquiring data in a given buffer solution. The QCM-D data were collected between 15 and 45 °C due to instrumental limitations. The reversibility of the collapse transition was checked. Because of the presence of a small hysteresis resulting from the large time constant needed for the stabilization of the QCM-D setup,[28] the frequency shift (Δf) and dissipation shift (ΔD) curves obtained upon heating and cooling, or upon increasing and decreasing the pH, are slightly different and were thus averaged.

All QCM-D data from a sample were merged in a single file containing the temperature and pH dependence of the brush. The data were then fitted by a procedure adapted from our previous work[28] based on Voinova et al.'s equations,[30] briefly described hereafter. The frequency shift and dissipation shift measured by the QCM-D are linked to the temperature- and pH-dependent thickness $h(T,\mathrm{pH})$, density $\rho(T,\mathrm{pH})$, shear viscosity $\eta(T,\mathrm{pH})$, and shear modulus $\mu(T,\mathrm{pH})$ of the polymer brush. In order to simplify the analysis, a relative swelling ratio α was defined as

$$\alpha(T,\mathrm{pH}) = \frac{h(T,\mathrm{pH})}{h^0} \quad (1)$$

where h is the thickness of the brush and h^0 its thickness in a reference collapsed state defined as T = 45 °C and pH = 3. The shear modulus μ and viscosity η of the polymer brush were

developed as Taylor's series of α truncated to first order:

$$\mu(\alpha) = \mu^0 + \dot{\mu}(\alpha - \alpha^0) \quad \text{and} \quad \eta(\alpha) = \eta^0 + \dot{\eta}(\alpha - \alpha^0) \quad (2)$$

where the superscript 0 is relative to the reference state. In these equations, μ^0, η^0, $\dot{\mu}$, and $\dot{\eta}$ are fittable coefficients, and $\alpha^0 = h^0/h^0 = 1$. Equation 2 effectively supposes that the swelling ratio affects linearly the viscoelasticity of the polymer brush in the limited range of the transition. A sigmoidal curve was used to describe α versus pH, and the parameters of the sigmoidal curve, i.e., its width, amplitude, baseline, and position, were taken as second- or third-order polynomial functions of T in order to couple the thermo- and pH-responses. The coefficients of these polynomial functions were also fittable parameters. $\mu(\alpha)$, $\eta(\alpha)$, and $\alpha(T,\mathrm{pH})$ were then used to describe the QCM-D data according to

$$\Delta f(T,\mathrm{pH}) \approx C_f \left[\frac{\eta_L(T)}{\delta_L(T)} + h^0 \alpha(T,\mathrm{pH}) \rho(\alpha) \omega - 2h^0 \alpha(T,\mathrm{pH}) \left(\frac{\eta_L(T)}{\delta_L(T)} \right)^2 \frac{\eta(\alpha)\omega^2}{\mu^2(\alpha) + \eta^2(\alpha)\omega^2} \right] \quad (3)$$

$$\Delta D(T,\mathrm{pH}) \approx C_D \left[\frac{\eta_L(T)}{\delta_L(T)} + 2h^0 \alpha(T,\mathrm{pH}) \left(\frac{\eta_L(T)}{\delta_L(T)} \right)^2 \frac{\mu(\alpha)\omega}{\mu^2(\alpha) + \eta^2(\alpha)\omega^2} \right] \quad (4)$$

where ω is the angular frequency of the considered harmonics. The constants $C_f = -(2\pi\rho_s h_s)^{-1}$ and $C_D = \omega\rho_s h_s$, where h_s is the thickness of the quartz crystal and ρ_s its density, can be determined easily and are considered to be temperature independent in our conditions. $\delta_L(T) = [2\eta_L(T)/\rho_L(T)\omega]^{1/2}[m]$ is the water viscous penetration depth where $\eta_L(T)$ and $\rho_L(T)$ are water viscosity and water density, respectively.

Infrared Spectroscopy. FT-IR absorbance spectra of the dry polymer brushes on silicon wafers were recorded with a Fourier transform infrared spectrometer (Nicolet Nexus 870). The transmission spectra of the pure copolymer brushes were obtained after subtraction of a silicon wafer reference. 128 scans were collected and averaged for each spectrum with a resolution of 8 cm^{-1}. Before each acquisition the chamber was purged with nitrogen for 20 min. The minimal thickness of the polymer brushes that could be characterized is ~30 nm.

The composition of the polymer brushes in MEO_2MA and MAA units was determined from the FT-IR spectra in the dry state. Because the infrared spectrum of the MAA units depends on their protonation state, all brushes were immersed in a sodium carbonate buffer solution at pH = 10 for 10 min, rinsed, and dried before measurement. According to the Lambert−Beer equation, the absorbance (A) is linearly related to the thickness of the dry polymer brushes (h^{dry}) by $A = \varepsilon c h^{\mathrm{dry}} \triangleq a h^{\mathrm{dry}}$, where ε is the extinction coefficient of the brush and c the molar concentration in monomer units. A decomposition of the infrared spectra in Voigt functions was used to integrate the absorbance of the two reference peaks specific to MEO_2MA or MAA moieties: the 1728 cm^{-1} peak associated with the asymmetrical stretching of the carbonyl group of MEO_2MA ($\delta_{\mathrm{as}}^{\mathrm{MEO_2MA}}$) and the 1554 cm^{-1} peak associated with the asymmetrical stretching of the carbonyl group of deprotonated MAA ($\delta_{\mathrm{as}}^{\mathrm{MAA}}$). From a series of measurements performed on pure homo-P(MEO_2MA) and pure homo-P(MAA) brushes of varying thickness (determined by ellipsometry), the a values were calibrated from the two reference absorbance peaks of P(MEO_2MA) and P(MAA): $a_{\mathrm{MEO_2MA}}(1728\ \mathrm{cm}^{-1}) = 0.008 \pm 0.001\ \mathrm{nm}^{-1}$ and $a_{\mathrm{MAA}}(1554\ \mathrm{cm}^{-1}) = 0.03 \pm 0.007\ \mathrm{nm}^{-1}$. For copolymer brushes, the relative composition was obtained from the area below the reference peaks, A_{1728} and A_{1554}, and the ellipsometric thickness of the dry brushes, h^{dry}, using

$$\frac{n_{\mathrm{MAA}}}{n_{\mathrm{MEO_2MA}}} = \frac{h^{\mathrm{dry}}_{\mathrm{MAA}}}{h^{\mathrm{dry}}_{\mathrm{MEO_2MA}}} \frac{\bar{V}_{\mathrm{MEO_2MA}}}{\bar{V}_{\mathrm{MAA}}} = \frac{A_{1554}}{A_{1728}} \frac{a_{\mathrm{MEO_2MA}}}{a_{\mathrm{MAA}}} \frac{\bar{V}_{\mathrm{MEO_2MA}}}{\bar{V}_{\mathrm{MAA}}} \quad (5)$$

where n_i is the number of moles of monomer i in the brush and $\bar{V}_i$ is its molar volume. $\bar{V}_{\mathrm{MEO_2MA}}/\bar{V}_{\mathrm{MAA}} \simeq 2.4$ was estimated from Van Krevelen's relationships.[31] The brush molar composition in MEO_2MA units was obtained as

$$\frac{n_{\mathrm{MEO_2MA}}}{n_{\mathrm{MEO_2MA}} + n_{\mathrm{MAA}}} = \left(1 + \frac{n_{\mathrm{MAA}}}{n_{\mathrm{MEO_2MA}}} \right)^{-1} \quad (6)$$

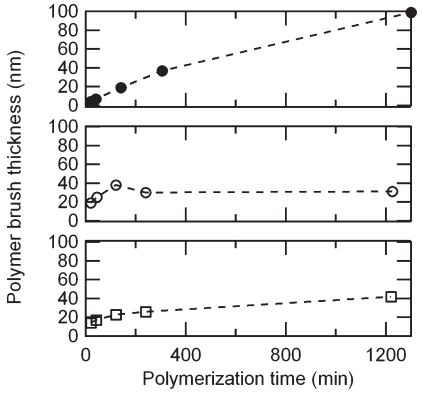

Figure 1. Examples of kinetics of P(MEO_2MA-*co*-MAA) brush growth (thickness versus polymerization time). The dashed lines serve as guides for the eye. The conditions of polymerization (monomers/bipy/CuCl/$CuCl_2$) (mmol) in H_2O:EtOH (mL) solution at pH = 9 are top (190/5/1.6/0.08) in 15:10; middle (152/5/1.6/0.08) in 22:22; and bottom (76/5/1.6/0.16) in 30:15.

Results and Discussion

Growth of the Copolymer Brushes. The synthesis of copolymer brushes containing acrylic acid units is an attractive way to generate pH- or salt-responsive surfaces or to introduce functional groups. However, the copolymerization of carboxylic acid-bearing moieties by ATRP is difficult because the acid groups deactivate the ligands used in ATRP by complexing them.[32] In most cases, a protected acid monomer such as *tert*-butyl methacrylate is thus copolymerized and then hydrolyzed to provide acid groups.[33] However, recent results indicate the possibility to polymerize methacrylic acid by ATRP at a basic pH.[34] Therefore, we investigated the growth of poly(di(ethylene glycol) methyl ether methacrylate-*co*-methacrylic acid), P(MEO_2MA-*co*-MAA), brushes by direct copolymerization in basic conditions. The copolymerization is performed from silicon substrates covered by an ATRP initiator silane monolayer in a water ethanol-based solution. In these conditions, the polymerization rates of the two homopolymers P(MAA) and P(MEO_2MA) are different; therefore, the pH of the solution, the relative concentrations of ethanol and water, and the concentrations in methacrylate monomers, catalyst, ligand, and deactivator were varied until a controlled copolymerization could be obtained with a growth rate compatible with desired brushes thicknesses. The polymer thickness is expected to be linear with time for a well-controlled living polymerization giving a

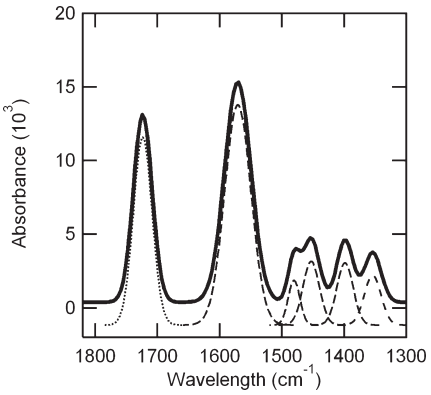

Figure 2. Infrared spectrum of a deprotonated P(MEO_2MA_{46}-*co*-MAA_{54}) brush of 72 nm thickness and decomposition of the signal in Voigt components (dotted lines refer to MEO_2MA units, dashed lines to MAA units). The signal from the bare substrate was subtracted.

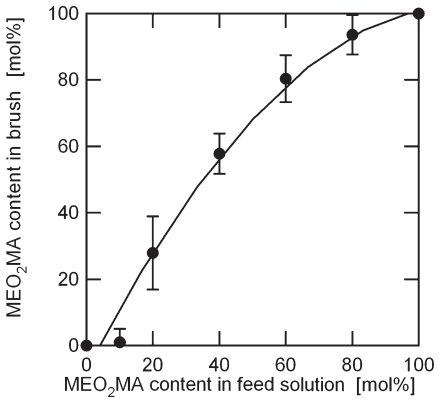

Figure 3. Composition of the copolymer brushes depending on the relative monomer content in the feed solution. The continuous line is the Mayo−Lewis equation with $r_{MEO_2MA} = 3.7$ and $r_{MAA} = 1$.

low polydispersity. Figure 1 shows three among many tested polymerization kinetics for P(MEO_2MA-*co*-MAA) brushes. As can be seen, conditions leading to a quasilinear increase of thickness with polymerization time can be found, provided the relative amounts of CuCl and $CuCl_2$ are properly tuned. It was also found that the methacrylate concentration and the amount of water in the feed solution influence the kinetics as well. In the sequel, we have selected conditions leading to linear growth of a copolymer brushes, corresponding to monomers/bipy/CuCl/$CuCl_2$ = 190/5/1.6/0.08 mmol, in a 15:10 vol:vol water:ethanol solution at pH 9.

Composition of the Copolymer Brushes. Because the composition of the polymer brushes could differ from the one of the feed solution, the brush compositions were measured by infrared spectroscopy (see Experimental Section). A typical infrared spectrum of a deprotonated comonomer brush is shown in Figure 2. The P(MEO_2MA) brushes exhibit a strong isolated peak at 1728 cm^{-1} corresponding to the asymmetrical stretching of the carbonyl group ($\delta_{as}^{PMEO_2MA}$). The infrared spectrum of the P(MAA) brushes depends on their protonation state.[35,36] At low pH, the acid units of P(MAA) brushes are protonated and form dimers involving intra- or intermolecular H-bonds. The asymmetrical stretching of the carbonyl group associated with this configuration is located at 1704 cm^{-1} and cannot be used to determine easily the copolymer composition because it overlaps with the $\delta_{as}^{PMEO_2MA}$ peak. At high pH, the acid groups of P(MAA) brushes are deprotonated, and the asymmetric stretching of the carbonyl shifts to ∼1500 cm^{-1} and splits into five peaks.[36] Here, the strong peak at 1554 cm^{-1} of deprotonated brushes was used to obtain the content in carboxylate anions. The composition of the copolymer brushes was computed from the thickness of the dry brush measured by ellipsometry and from the integrated absorbances at 1554 and 1728 cm^{-1} as described in the Experimental Section.

The actual composition of the copolymer brushes is shown in Figure 3 as a function of the composition of the feed solution. The copolymer tends to be richer in MEO_2MA units than the feed solution, indicating preferential polymerization of MEO_2MA compared to MAA. Infrared spectra were also acquired on samples at different polymerization times. The composition of the copolymer brushes was found to be essentially time-independent.

The reactivity ratio is defined as $r_i = k_{ii}/k_{ij}$ where k_{ij} is the reaction rate constant of the addition of monomer j on a growing chain terminated by a monomer unit i. The data of Figure 3 was modeled by the Mayo−Lewis equation,[37] providing $r_{MEO_2MA} = 3.7$ and $r_{MAA} = 1$. This is reasonably close to previous results obtained for free radical copolymerization in solution for the same monomers ($r_{MEO_2MA} = 3.6$ and $r_{MAA} = 2$).[38] From these reactivity ratios, we have computed that,[38] for a 70/30 MEO_2MA/MAA composition of the feed leading to the growth of P(MEO_2MA_{86}-*co*-MAA_{14}) brushes, the distribution of MEO_2MA sequence lengths is broad and peaks at ∼9 units, whereas the one of MAA is sharp and peaks at 1 unit, corresponding to blocks of ∼1−3 MAA units randomly interspersed in the chains. Likewise, for P(MEO_2MA_{96}-*co*-MAA_4) brushes, MAA blocks of ∼1−2 units are randomly inserted in the P(MEO_2MA) chains with a broad distribution of MEO_2MA sequence lengths peaking at 25 units.

Monitoring the Collapse of Thermo-Responsive Brushes and pH-Responsive Brushes by QCM-D. The collapse transition was characterized by QCM-D. This method is based on the monitoring of the resonance frequency of a piezoelectric sensor. A quartz crystal placed between two electrodes is excited by an oscillating electric field and begins to vibrate when the frequency of this electrical field is close to its resonance frequency. The resonance frequency depends on parameters of the quartz crystal such as its thickness, density, and elastic shear modulus. The addition or modification of an adsorbed layer alters the resonance frequency of the quartz crystal, resulting in a shift Δf compared to the bare crystal. In addition to resonance frequencies, the dissipation energy is measured by switching off the exciting electric field. The part of accumulated energy lost at each oscillation of the system corresponds to the dissipation energy, which, compared to the bare crystal, provides the dissipation shift ΔD. For a viscoelastic film measured in solution, the values of Δf and ΔD can be related to the increment of mass Δm and the viscoelastic modulus of the deposited layer.[39−41] QCM-D is frequently used to monitor the growth of thin films of adsorbed macromolecules on a surface. But QCM-D is also an interesting characterization method to monitor the swelling/collapsing process of a responsive polymer brush.[27] The thermo-collapse transition of responsive polymer brushes has been actually investigated before by QCM-D.[28,42,43]

The lower critical solution temperature of P(MEO_2MA) in water is 26 °C.[44] When grafted from a substrate, P(MEO_2MA) brushes exhibit a *bulk* collapse transition occurring over a temperature range of ∼15 °C centered at about 22 °C and a collapse transition of their *outer surface* at 32 °C.[28] Typical QCM-D data for our P(MEO_2MA) brushes are shown in Figure 4a. Over the whole investigated temperature range, the frequency shift Δf exhibits a continuously increasing trend with temperature. This progressive increase

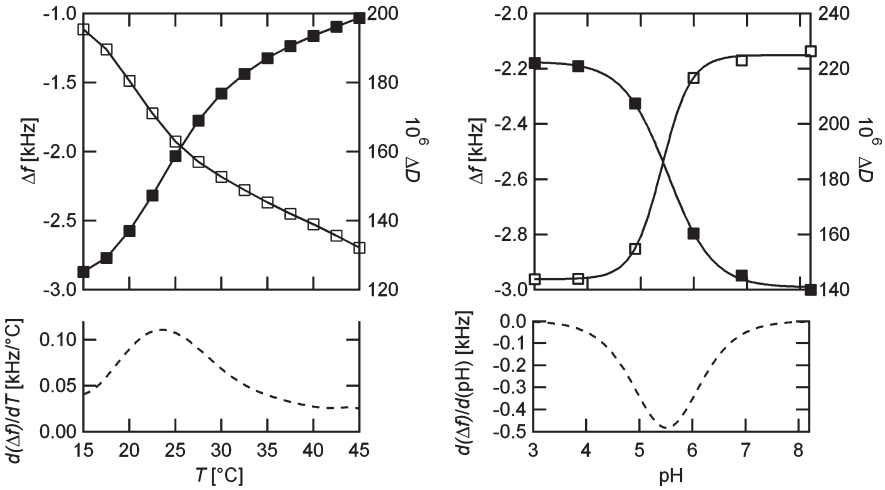

Figure 4. (a) Frequency and dissipation shift (Δf and ΔD) of a P(MEO_2MA) brush measured by QCM-D in water for increasing temperatures. The dry thickness of the brush is ~92 nm. The bottom panel provides the first derivative of Δf with temperature, allowing to spot easily the collapse transition temperature. (b) Δf and ΔD of a P(MAA) brush depending on the pH of the buffer solution (concentration of 0.05 M and ionic strength of 0.2 M). The dry thickness of the P(MAA) brush is ~65 nm. The continuous lines are sigmoidal fits. The bottom panel is the first derivative of Δf versus pH. The shifts are relative to the resonance frequency of the bare sensor at 22 °C in air. Error bars are smaller than the size of the symbols.

results from the decreasing viscosity and density of water with temperature. At ~22 °C, Δf undergoes gradually a change of curvature (inflection point) due to the collapse of the P(MEO_2MA) brush, which leads to a decreasing brush thickness, a loss of water, and a change in the viscoelastic properties of the layer. Likewise, the decreasing trend of ΔD over the whole probed temperature range is due to the decrease of water viscosity and density. The change of slope of ΔD around 22 °C is associated with the formation of the more rigid collapsed layer.[21,45]

The effect of pH on the swelling behavior of P(MAA) brushes in buffer solutions was also investigated by QCM-D measurements. Figure 4b shows the frequency and dissipation shifts of QCM-D sensors covered by P(MAA) brushes in solutions of different pH but of identical ionic strength. At low and high pH, Δf and ΔD are nearly pH-independent. In the intermediate pH region from 5 to 6, which corresponds to the pH of transition of P(MAA), the frequency shift decreases strongly with pH whereas the dissipation increases, suggesting an increasing thickness and a change of viscoelasticity associated with the switching from a rigid collapsed to a softer swollen state. At low pH, the carboxylic groups of the polymer chains form intra- or interchain hydrogen bonds, and the brush is less hydrophilic. By increasing the pH, the degree of ionization of the brushes increases until the P(MAA) chains are fully ionized at pH ≅ 8, converting to a more hydrated polymer brush.

The QCM-D data thus provide access to the pH of transition of the polyacid brush, which can be obtained by taking the maximum of the first derivative of Δf versus pH. For our P(MAA) brushes, the transition pH is around 5.5. The transition of P(MAA) brushes from a neutral to an ionized state was theoretically investigated before and by other experimental techniques. The transition was reported to occur in a pH range from 6 to 9 depending on molar mass, grafting density, and ionic strength.[46−51] The transition pH of polyacid brushes is expected to be higher than the one of the same polymer in solution. Indeed, the high charge density inside polymer brushes generates an electrostatic potential which prevents further ionization. At a given pH, the degree of dissociation of the polyelectrolytes inside the brushes is then lower than the one of free chains in dilute solution. This phenomenon is more important for a higher grafting density or a lower salt concentration.[52,53] In a solution of high ionic strength, the electrostatic charges of the brushes are screened by the free ions of the salt, and the degree of ionization in the brush becomes similar to the one of free chains.[49] Comparing our experimental conditions (ionic strength: 0.2 M; estimated grafting density of the polymer chains: ~0.3 chain/nm^2) to the theoretical models of Zhulina, Birshtein, and coworkers,[50,53] our P(MAA) brushes should belong to the salted brush regime, meaning that the degree of ionization inside the brushes should be similar to the one of free P(MAA) chains, as indeed observed here. It is interesting to note how efficient the QCM-D technique is for titrating the brushes, which opens real perspective for thorough studies of polyacid brushes. This is not, however, the purpose of the present study, which will concentrate in the sequel on the pH control of the thermal collapse in the copolymer brushes.

The influence of grafting density on the temperature- and pH-induced collapse transitions was also investigated, by using silanization solutions consisting of a mixture of the ATRP silane initiator and of a diluting inert silane. For a dilution by a factor of 2, the transition pH of P(MAA) brushes was decreased by 0.1, whereas the collapse temperature of P(MEO_2MA) brushes increased by 1 °C only. When the ATRP silane was diluted by a factor of 20, the collapse transition temperature of the P(MEO_2MA) brush was raised by ~6 °C, whereas the transition pH of P(MAA) brushes was decreased by 0.2. This indicates that the collapse transitions are not strongly affected by the grafting density, at least in the range of high grafting densities such as used here.

Thermo- and pH-Collapse Transition of Copolymer Brushes. Figure 5a shows the collapse transition temperature of P(MEO_2MA-*co*-MAA) brushes measured by QCM-D in Milli-Q water (pH = 5.5) for different amounts of MAA in the brush varying from 0 to 14 mol %. The transition is defined heuristically, as was done before,[28] by taking the inflection point of $\Delta f(T)$. For P(MEO_2MA) brushes, the thermal collapse of the bulk of the brush happens at ~22 °C, in agreement with previous results.[28] Upon copolymerization with MAA units, the thermal collapse shifts to lower temperatures. 14% of MAA units in the brushes decrease the average collapse temperature by 5 °C when pH = 5.5. Carboxylic acid groups in the brushes form hydrogen bonds with the ether or acid groups. The induced diminution of

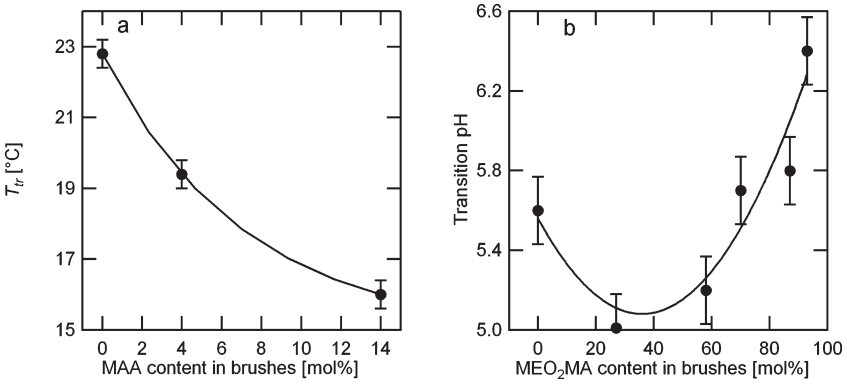

Figure 5. (a) Collapse transition temperature T_{tr} of P($MEO_2MA_{(1-y)}$-*co*-MAA_y) brushes depending on the brush composition y, measured in water at pH 5.5. (b) pH at which P($MEO_2MA_{(1-y)}$-*co*-MAA_y) brushes collapse in water at 22 °C, i.e., transition pH, depending on the brush composition y. Error bars were computed from the standard deviation of the data obtained on the third, fifth, and seventh overtones.

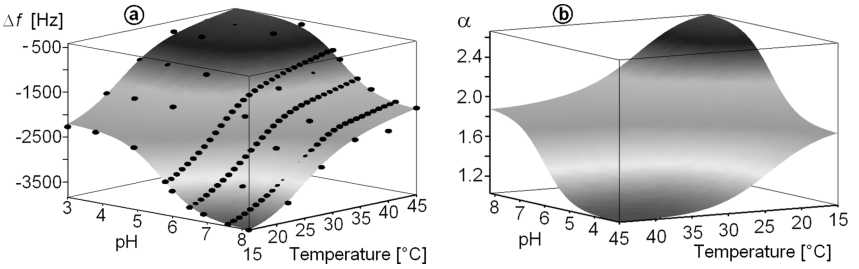

Figure 6. (a) Frequency shift of a P(MEO_2MA_{86}-*co*-MAA_{14}) brush measured by QCM-D in different buffer solutions at several temperatures. The experimental data (black dots) are fitted as explained in the Experimental Section (gray surface). The shifts are relative to the resonance frequency of the bare sensor at 22 °C in air. (b) Three-dimensional map of the relative swelling ratio (see text for definition) of the brush shown in (a), as obtained from the fit.

hydrogen bonding between water and copolymer chains reduces the hydrophilicity of the brushes and consequently results in a lower collapse temperature.

In Figure 5b, the pH at which P(MEO_2MA-*co*-MAA) copolymer brushes collapse is shown for different compositions at 22 °C in buffer solutions of 0.2 M ionic strength. The collapse pH, i.e., the transition pH, is defined as the inflection point of Δf(pH) curves. P(MAA) brushes exhibit a transition pH around 5.5. A small addition of MEO_2MA units in the copolymer brushes decreases the transition pH. The minimum is observed around 40% of MEO_2MA units. For larger amounts of MEO_2MA units, the transition pH increases with MEO_2MA content. The addition of a few MEO_2MA monomer units in the copolymer brushes induces a dilution of carboxylic acid groups. Therefore, the degree of ionization at a given pH increases because the average distance between two neighboring ionized acid groups increases. This explains the lower transition pH for low MEO_2MA contents. For a larger amount of MEO_2MA, the complex interplay between the thermal and pH collapses is responsible for the variation of the transition pH with MEO_2MA content as was suggested before for free polymer chains in solution.[54]

To investigate in more detail this interplay, we have analyzed simultaneously the pH- and temperature-dependence of the QCM-D response. Figure 6a is the frequency shift of P(MEO_2MA_{86}-*co*-MAA_{14}) brushes depending on temperature and pH. The Δf variation between the minimum (T = 15 °C, pH = 8) and the maximum (T = 45 °C, pH = 3) equals 3350 Hz, which corresponds to a modification of the polymer brush from a well swollen state (T = 15 °C, pH = 8) to a collapsed state (T = 45 °C, pH = 3) induced by both temperature and pH. A similar graph could be obtained for P(MEO_2MA_{96}-*co*-MAA_4) brushes (data not shown), which exhibit the same behavior. Once taking into account the effect of the diminution of the water viscosity and density on Δf, the amplitude of the thermo-collapse transition along a given iso-pH line appears to be slightly smaller than the amplitude of the pH-collapse transition along a given isothermal line for the P(MEO_2MA_{86}-*co*-MAA_{14}) brush shown in Figure 6a. This is because the electrostatic forces appearing due to the ionization of MAA units are stronger and induce larger conformational changes than the variation in the number of hydrogen bonds which controls the thermo-collapse transition.

Bidimensional Maps of the pH- and Temperature-Responses of Adaptive Polymer Brushes. In order to obtain a more direct view of the collapse transition of adaptive brushes, a model was fit to the experimental data Δf(pH,T), allowing us to retrieve the swelling ratio α(pH,T) = h(pH,T)/h^0 relative to a reference state taken here as T = 45 °C and pH = 3. This reference state is the most collapsed state of the brushes of our study, as can be checked by inspecting Figure 6a. A typical fit is shown as the gray surface in Figure 6a, corresponding to the relative swelling ratio of Figure 6b. One should be aware that α is an acoustic swelling ratio allowing to get access more easily to the conformational changes occurring in the brush, but that it should not be taken as an absolute determination of the thickness of the brush, given the simplicity of the model.[28] The details of the mathematical model used to extract α(T,pH) are given in the Experimental Section. Color maps of α are presented in Figure 7 for brushes containing 4 and 14 mol % MAA, together with isoswelling contour lines including the half-collapse lines (dashed) which coincide with the brushes being halfway between their swollen and collapsed states.

The swelling of pure P(MAA) and pure P(MEO_2MA) brushes was also investigated, and their half-collapse lines

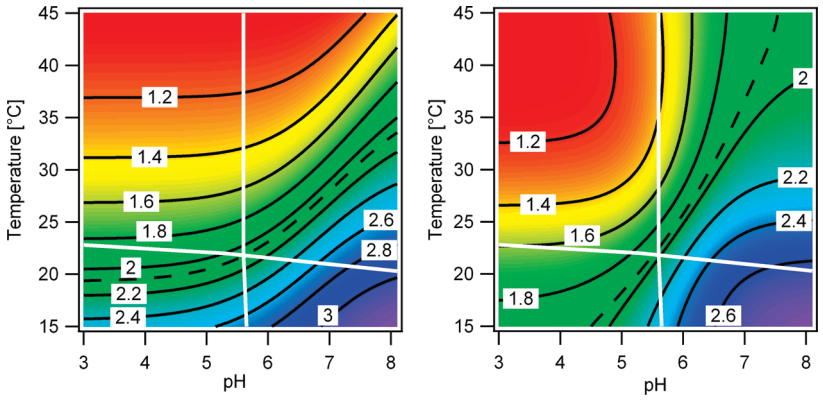

Figure 7. Relative swelling ratio, $\alpha(T,\mathrm{pH})$, of a P(MEO_2MA_{96}-*co*-MAA_4) brush (left) and of a P(MEO_2MA_{86}-*co*-MAA_{14}) brush (right). Black curves are isoswelling contour curves; the black dashed curves are the half-swelling curves; the thick white lines represent the half-swelling curves of pure P(MEO_2MA) and P(MAA) brushes, respectively.

are displayed in white in Figure 7. For a pure P(MAA) brush, which is almost insensitive to temperature in the probed range, the half-collapse line is a vertical line in Figure 7; for a pure P(MEO_2MA) brush, which should not be not sensitive to pH, the half-collapse line is indeed nearly horizontal. In contrast, the copolymer brushes displayed in Figure 7 have tilted half-collapse lines, evidencing the strong coupling between their pH- and temperature-dependence. The brush containing 4 mol % of MAA (Figure 7, left) displays a pH-independent regime for pH < 5, indicating that sush brushes should be considered as thermoresponsive systems with a collapse modulated by pH in the 5−8 range. Conversely, the brush containing 14 mol % MAA (Figure 7, right) tends to be less temperature-sensitive, suggesting that this brush should preferably be considered as a pH-responsive brush with a transition pH modulated by temperature below ∼35 °C. For 4% MAA, the temperature of the thermo-collapse transition varies from 19 to 34 °C, depending on pH in the 5−8 range. By increasing the MAA content, the thermo-collapse transition depends even more on pH and can be tuned over an even larger temperature range. Conversely, the pH-collapse transition displays a stronger temperature dependence for a lower MAA content in the copolymer brushes.

Clearly, the range of MAA contents for which the brushes exhibit adaptive behavior is biased toward low MAA contents due to the strength of the electrostatic interaction compared to the hydrophobic interaction. Maps such as shown in Figure 7 illustrate the complexity of adaptive brushes as well as the need to analyze simultaneously the response of the brush to both stimuli to obtain a significant picture. In this context, it is noteworthy that the half-collapse points determined over the bidimensional maps are not identical to the half-collapse determined along a single iso-pH or isothermal line. This explains why graphs such as shown in Figure 5b should be interpreted with caution. The maps also show how sensitive a thermo-responsive brush is even to small amounts of ionizable groups and provide an elegant way to determine the steepest slope in (pH, *T*) space, when large variation of properties are desired. They also indicate the pathway to follow in (pH, *T*) space if the brush has to collapse in a series of steps, e.g., when the brush is used for actuation.[10]

Conclusions

P(MEO_2MA-*co*-MAA) brushes were grown by ATRP from silicon surfaces, and the reactivity ratios of the monomers were measured by FT-IR. Random copolymers are obtained with brushes exhibiting a linear growth with time, when brushes are grown at pH 9. For two different compositions of the polymer brushes, a characterization of the thermo- and pH-collapse transition was performed by QCM-D measurements. The QCM-D, already used previously to monitor thermo-collapse transitions, appears also to be an efficient way to monitor the pH-collapse transition of pH-responsive brushes.

Pure P(MEO_2MA) brushes display a collapse transition around 22 °C in water only marginally affected by pH, and P(MAA) brushes exhibit a transition pH of ∼5.5, independent of temperature. In addition, the transitions of these homopolymer brushes are not strongly dependent on grafting density in the range of high grafting densities. In contrast, P(MEO_2MA-*co*-MAA) brushes exhibit adaptivity and undergo a collapse transition modulated by either temperature or pH from a swollen state at low temperature and high pH to a collapsed state at high temperature and low pH. According to the swelling ratio data, the copolymer brushes in the transition region exhibit an intermediate state between fully collapsed and swollen. The 2D diagrams of swelling ratio computed from the QCM-D data illustrate the sensitivity of the adaptive behavior to brush composition. Copolymer brushes with very low MAA content behave as pH-modulated thermoresponsive brushes, while a brush containing 14% of MAA already behaves more as a temperature-modulated pH-responsive brush. Such 2D maps also allow to select temperature and pH conditions to follow the steepest gradient slope of the swelling ratio. Obtaining maps by QCM-D is relatively easy and should find widespread use in the future, given the interest of adaptive brushes for applications such as medical devices able to adapt to local temperature and pH or for the fabrication of smart actuators.

Acknowledgment. We are grateful to Karine Glinel (UCLouvain) and Wilhelm Huck (Cambridge, UK) for their critical input at various stages of this work, to Christine Dupont (UCLouvain) for access to the QCM-D apparatus, and to Peter Hensenne and Olivier Riant (UCLouvain) for helping synthesizing the silane initiator. B.N. is Senior Research Associate of the F.R.S.-FNRS. Financial support was provided by the Communauté Française de Belgique (ARC 06-11/339), the Belgian Federal Science Policy (IAP-PAI P6/27), the F.R.S.-FNRS, and the Wallonia Region (Nanotic-Feeling).

References and Notes

(1) Jones, D. M.; Smith, J.; Huck, W. T. S.; Alexander, C. *Adv. Mater.* **2002**, *14*, 1130–1134.
(2) Zhou, F.; Huck, W. T. S. *Phys. Chem. Chem. Phys.* **2006**, *8*, 3815–3823.
(3) LeMieux, M. C.; Peleshanko, S.; Anderson, K. D.; Tsukruk, V. V. *Langmuir* **2007**, *23*, 265–273.

(4) Tokareva, I.; Minko, S.; Fendler, J. H.; Hutter, E. *J. Am. Chem. Soc.* **2004**, *126*, 15950–15951.
(5) Yu, C.; Mutlu, S.; Selvaganapathy, P.; Mastrangelo, C. H.; Svec, F.; Frechet, J. M. J. *Anal. Chem.* **2003**, *75*, 1958–1961.
(6) Kataoka, D.; Troian, S. *Nature* **1999**, *402*, 794–797.
(7) Kumar, A.; Srivastava, A.; Galaev, I. Y.; Mattiasson, B. *Prog. Polym. Sci.* **2007**, *32*, 1205–1237.
(8) Miyata, T.; Asami, N.; Uragami, T. *Nature* **1999**, *399*, 766–769.
(9) Aksay, I.; Trau, M.; Manne, S.; Honma, I.; Yao, N.; Zhou, L.; Fenter, P.; Eisenberger, P.; Gruner, S. *Science* **1996**, *273*, 892–898.
(10) Santer, S.; Ruhe, J. *Polymer* **2004**, *45*, 8279–8297.
(11) Ebara, M.; Aoyagi, T.; Kikuchi, A.; Sakai, K.; Okano, T. *Biomacromolecules* **2004**, *5*, 505–510.
(12) Wischerhoff, E.; Uhlig, K.; Lankenau, A.; Borner, H. G.; Laschewsky, A.; Duschl, C.; Lutz, J. F. *Angew. Chem., Int. Ed.* **2008**, *47*, 5666–5668.
(13) Lee, H.; Pietrasik, J.; Matyjaszewski, K. *Macromolecules* **2006**, *39*, 3914–3920.
(14) Yamamoto, S.; Pietrasik, J.; Matyjaszewski, K. *Macromolecules* **2008**, *41*, 7013–7020.
(15) Chen, G.; Hoffman, A. S. *Nature* **1995**, *373*, 49–52.
(16) Plamper, F. A.; Ruppel, M.; Schmalz, A.; Borisov, O.; Ballauff, M.; Muller, A. H. E. *Macromolecules* **2007**, *40*, 8361–8366.
(17) Liu, Q.; Yu, Z.; Ni, P. *Colloid Polym. Sci.* **2004**, *282*, 387–393.
(18) Butun, V.; Armes, S. P.; Billingham, N. C. *Polymer* **2001**, *42*, 5993–6008.
(19) Peng, T.; Cheng, Y. L. *Polymer* **2001**, *42*, 2091–2100.
(20) Yoo, M.; Sung, Y.; Cho, C.; Lee, Y. *Polymer* **1997**, *38*, 2759–2765.
(21) Luzinov, I.; Minko, S.; Tsukruk, V. V. *Prog. Polym. Sci.* **2004**, *29*, 635–698.
(22) Gersappe, D.; Fasolka, M.; Israels, R.; Balazs, A. C. *Macromolecules* **2002**, *28*, 4753–4755.
(23) Jonas, A. M.; Glinel, K.; Oren, R.; Nysten, B.; Huck, W. T. S. *Macromolecules* **2007**, *40*, 4403–4405.
(24) Vihola, H.; Laukkanen, A.; Valtola, L.; Tehnhu, H.; Hirnoven, J. *Biomaterials* **2005**, *26*, 3055–3064.
(25) Glinel, K.; Jonas, A. M.; Jouenne, T.; Leprince, J.; Galas, L.; Huck, W. T. S. *Bioconjugate Chem.* **2009**, *20*, 71–77.
(26) Laloyaux, X.; Fautre, E.; Blin, T.; Purohit, V.; Leprince, J.; Jouenne, T.; Jonas, A. M.; Glinel, K. *Adv. Mater.*, in press.
(27) Domack, A.; Prucker, O.; Ruhe, J.; Johannsmann, D. *Phys. Rev. E* **1997**, *56*, 680.
(28) Laloyaux, X.; Mathy, B.; Nysten, B.; Jonas, A. M. *Langmuir* **2010**, *26*, 838–847.
(29) Jonas, A. M.; Hu, Z.; Glinel, K.; Huck, W. T. S. *Macromolecules* **2008**, *41*, 6859–6863.
(30) Voinova, M.; Rodahl, M.; Jonson, M.; B., K. *Phys. Scr.* **1999**, *59*, 391–396.
(31) van Krevelen, D. *Properties of Polymers: Correlations with Chemical Structure*, 1st ed.; Elsevier: Amsterdam, 1972.
(32) Matyjaszewski, K.; Xia, J. *Chem. Rev.* **2001**, *101*, 2921–2990.
(33) Davis, K.; Matyjaszewski, K. *Macromolecules* **2000**, *33*, 4039–4047.
(34) Tugulu, S.; Barbey, R.; Harms, M.; Fricke, M.; Volkmer, D.; Rossi, A.; Klok, H. A. *Macromolecules* **2007**, *40*, 168–177.
(35) Hu, H.; Saniger, J.; Garcia-Alejandre, J.; Castano, V. M. *Mater. Lett.* **1991**, *12*, 281–285.
(36) Konradi, R.; Ruhe, J. *Macromolecules* **2004**, *37*, 6954–6961.
(37) Mayo, F. R.; Lewis, F. M. *J. Am. Chem. Soc.* **1944**, *66*, 1594–1601.
(38) Smith, B. L.; Klier, J. *J. Appl. Polym. Sci.* **1998**, *68*, 1019–1025.
(39) Granstaff, V. E.; Martin, S. J. *J. Appl. Phys.* **1994**, *75*, 1319–1329.
(40) Nakamoto, T.; Moriizumi, T. *Jpn. J. Appl. Phys.* **1990**, *29*, 963–969.
(41) Johannsmann, D. *Phys. Chem. Chem. Phys.* **2008**, *10*, 4516–4534.
(42) Liu, G.; Zhang, G. *J. Phys. Chem. B* **2005**, *109*, 743–747.
(43) Annaka, M.; Yahiro, C.; Nagase, K.; Kikuchi, A.; Okano, T. *Polymer* **2007**, *48*, 5713–5720.
(44) Lutz, J. F. *J. Polym. Sci., Part A: Polym. Chem.* **2008**, *46*, 3459–3470.
(45) Yuk, S. H.; Cho, S. H.; Lee, S. H. *Macromolecules* **1997**, *30*, 6856–6859.
(46) Sanjuan, S.; Tran, Y. *Macromolecules* **2008**, *41*, 8721–8728.
(47) Parnell, A. J.; Martin, S. J.; Dang, C. C.; Geoghegan, M.; Jones, R. A. L.; Crook, C. J.; Howse, J. R.; Ryan, A. J. *Polymer* **2009**, *50*, 1005–1014.
(48) Lee, H.; Boyce, J. R.; Nese, A.; Sheiko, S. S.; Matyjaszewski, K. *Polymer* **2008**, *49*, 5490–5496.
(49) Currie, E. P. K.; Sieval, A. B.; Fleer, G. J.; Stuart, M. A. C. *Langmuir* **2000**, *16*, 8324–8333.
(50) Lyatskaya, Y. V.; Leermakers, F. A. M.; Fleer, G. J.; Zhulina, E. B.; Birshtein, T. M. *Macromolecules* **2002**, *28*, 3562–3569.
(51) Biesalski, M.; Johannsmann, D.; Ruhe, J. *J. Chem. Phys.* **2002**, *117*, 4988–4994.
(52) Israels, R.; Leermakers, F. A. M.; Fleer, G. J. *Macromolecules* **2002**, *27*, 3087–3093.
(53) Zhulina, E. B.; Birshtein, T. M.; Borisov, O. V. *Macromolecules* **2002**, *28*, 1491–1499.
(54) Jones, J. A.; Novo, N.; Flagler, K.; Pagnucco, C. D.; Carew, S.; Cheong, C.; Kong, X. Z.; Burke, N. A. D.; Stover, H. D. H. *J. Polym. Sci., Part A: Polym. Chem.* **2005**, *43*, 6095–6104.